

Boundary Effects on Spectral Properties of Interacting Electrons in One Dimension

Sebastian Eggert, Henrik Johannesson, and Ann Mattsson

Institute of Theoretical Physics, Chalmers University of Technology and Göteborg University, S-412 96 Göteborg, Sweden
(Received 9 November 1995)

The single electron Green's function of the one-dimensional Tomonaga-Luttinger model in the presence of open boundaries is calculated with bosonization methods. We show that the critical exponents of the local spectral density and of the momentum distribution change in the presence of a boundary. The well understood universal bulk behavior always crosses over to a boundary dominated regime for small energies or small momenta. We show this crossover explicitly for the large- U Hubbard model in the low-temperature limit. Consequences for photoemission experiments are discussed.

PACS numbers: 71.10.Pm, 71.27.+a

There is currently great interest in "Luttinger liquid physics" [1,2], sparked by a new generation of experiments on low-dimensional electron structures. Examples include measurements of the point contact tunneling conductance between two fractional quantum Hall edge channels [3] and high-resolution photoemission studies of quasi-one-dimensional metals [4,5]. Additional interest stems from the fact that the Luttinger liquid—i.e., the low-energy, long-wavelength physics of interacting electrons in one dimension (1D)—provides us with the only known non-Fermi liquid phase with unbroken symmetry. For this reason the notion of a "Luttinger liquid" (LL) has played a prominent role in studies of generic features of correlated electron systems, and it has been suggested that some of its properties (e.g., anomalous propagators, spin-charge separation) carry over to higher dimensions [6].

So far little attention has been paid to the effect of *boundaries* on the spectral properties of Luttinger liquids (except in the context of spin chains [7]). This is surprising since boundary effects are bound to be important in several of the proposed laboratory realizations. For example, in a recent series of experiments on the Bechgaard salts $(\text{TMTSF})_2X$ (X is a counterion), the He I and II photoemission spectra were measured in the metallic phase [5]. This class of materials is known to exhibit strong electron correlations and is a prime candidate for LL behavior. The experimental results suggest an anomalous suppression of the spectral weight close to the Fermi level. It was argued in [5] that consistency with the LL scenario requires long-range electron-electron interactions, but as we will show here, boundary effects also deplete the spectral weight and may influence the observed data.

Specifically, we have examined the effect of an open boundary on the local single-particle spectral density of a spinful LL. We have also studied the momentum distribution in a finite system with open boundary conditions. In both cases we observe a strong influence from the boundaries, which causes novel scaling behavior with energies and momenta close to the Fermi level.

As our model we take an extended version of the Tomonaga-Luttinger (TL) Hamiltonian, describing the

low-energy limit of locally interacting 1D electrons [2,8], defined by the Hamiltonian density

$$\begin{aligned} \mathcal{H} = v_F \left[\psi_{L,\sigma}^\dagger i \frac{d}{dx} \psi_{L,\sigma} - \psi_{R,\sigma}^\dagger i \frac{d}{dx} \psi_{R,\sigma} \right] \\ + g_1 J_L^\sigma J_R^{-\sigma} + g_2 J_L^\sigma J_R^\sigma + g_3 (J_L^\sigma J_L^{-\sigma} + J_R^\sigma J_R^{-\sigma}) \\ + g_4 \psi_{L,\sigma}^\dagger \psi_{R,\sigma} \psi_{R,-\sigma}^\dagger \psi_{L,-\sigma}. \end{aligned} \quad (1)$$

Here $J_{L/R}^\sigma \equiv: \psi_{L/R,\sigma}^\dagger \psi_{L/R,\sigma} :$ are the chiral Fermion currents of the left and right moving components of the electron field $\Psi_\sigma(x)$, expanded about the Fermi points $\pm k_F$: $\Psi_\sigma(x) = e^{-ik_F x} \psi_{L,\sigma}(x) + e^{ik_F x} \psi_{R,\sigma}(x)$. The Hamiltonian (1) describes left and right moving relativistic Fermions in (1+1) dimensions which interact via forward scattering without spin flip (g_1, g_2 , and g_3) or with spin flip (g_4). "Umklapp" processes are suppressed away from half-band filling, so this model provides a complete picture of possible local interactions in this case. (Trivial forward scattering terms which can be absorbed by redefining the Fermi velocity have not been explicitly written out.)

The TL Hamiltonian is conveniently bosonized [9] by introducing charge and spin currents and the corresponding bosons ϕ_c and ϕ_s with conjugate momenta Π_c and Π_s , respectively:

$$J_L^{c/s} \equiv \frac{1}{\sqrt{2}} (J_L^\dagger \pm J_L^l) = \frac{1}{\sqrt{4\pi}} (\Pi_{c/s} + \partial_x \phi_{c/s}), \quad (2)$$

and accordingly for right movers. The resulting theory describes separate spin and charge excitations moving with velocities $v_c = \frac{v_F}{2} + \frac{g_3}{2\pi}$ and $v_s = \frac{v_F}{2} - \frac{g_3}{2\pi}$, respectively:

$$\begin{aligned} \mathcal{H} = \sum_{\nu=s,c} \left\{ v_\nu [(\partial_x \phi_\nu)^2 + \Pi_\nu^2] + \frac{g_\nu}{4\pi} [(\partial_x \phi_\nu)^2 - \Pi_\nu^2] \right\} \\ + g_4 \times \text{const} \times \cos \sqrt{8\pi} \phi_s, \end{aligned} \quad (3)$$

where $g_c = g_1 + g_2$ and $g_s = g_2 - g_1$. The charge interaction g_c can be absorbed into the free Hamiltonian by a simple rescaling of the charge boson, but the spin interactions g_s and g_4 obey Kosterlitz-Thouless renormalization group equations [10] with flow lines along hyperbolas $g_s^2 - g_4^2 = \text{const}$ (to lowest order). For $g_s > -|g_4|$ the

spin sector develops a gap in the low energy, long wavelength limit, but for $g_s < -|g_4|$ the system flows to a stable fixed point $g_s^* = -\sqrt{g_s^2 - g_4^2}$, $g_4^* = 0$. For $g_s = -|g_4|$ the interaction corresponds to one single marginally irrelevant operator, so that $g_s^* = g_4^* = 0$. If the flow to a stable fixed point occurs, we can rescale the bosons by a canonical transformation to obtain a free theory ($\nu = s, c$)

$$\phi_\nu \rightarrow K_\nu \phi_\nu, \quad \Pi_\nu \rightarrow \Pi_\nu / K_\nu, \quad (4)$$

where to first order in the coupling constants

$$K_s^2 = 1 - g_s^*/4\pi v_s, \quad K_c^2 = 1 - g_c/4\pi v_c. \quad (5)$$

We now consider a semi-infinite system with an *open* boundary condition at the origin and thus require the electron field $\Psi_\sigma(x)$ to vanish at $x = 0$. This implies $\psi_{L,\sigma}(0) = -\psi_{R,\sigma}(0)$, or in terms of the bosons $\phi_{L,c}(0) = -\phi_{R,c}(0) + \frac{\sqrt{\pi}}{2} K_c^{-1}$ and $\phi_{L,s}(0) = -\phi_{R,s}(0)$, which allows an analytic continuation of the left movers onto the negative half axis in terms of right movers

$$\phi_{L,\nu}(x, t) = -\phi_{R,\nu}(-x, t) + \text{const}, \quad x < 0 \quad (6)$$

($\nu = s, c, \text{const} = 0, \frac{\sqrt{\pi}}{2} K_c^{-1}$). We can therefore describe the theory in terms of left movers only which live on the full complex plane *without* an explicit boundary condition. Using this formalism, the single electron Green's function can be calculated in a straightforward way:

$$\begin{aligned} \langle \Psi_\sigma^\dagger(x, t) \Psi_\sigma(y, 0) \rangle &= e^{ik_F(x-y)} G(x, y, t) \\ &+ e^{-ik_F(x-y)} G(-x, -y, t) \\ &- e^{ik_F(x+y)} G(x, -y, t) \\ &- e^{-ik_F(x+y)} G(-x, y, t), \quad (7) \end{aligned}$$

where the chiral Green's function $G(x, y, t)$ is a product of spin and charge contributions

$$\begin{aligned} G(x, y, t) &\propto \prod_{\nu=c,s} (v_\nu t + x - y)^{-(K_\nu + K_\nu^{-1})^2/8} \\ &\times (v_\nu t - x + y)^{-(K_\nu - K_\nu^{-1})^2/8} \\ &\times \left(\frac{|4xy|}{[v_\nu^2 t^2 - (x + y)^2]} \right)^{(K_\nu^{-2} - K_\nu^2)/8}. \quad (8) \end{aligned}$$

Here, x and y denote the distance from the boundary ($x = 0$) and the time carries an implicit ultraviolet cutoff $t - i\epsilon$. We can see that in the limit $xy \gg |(x - y)^2 - v_\nu^2 t^2|$ the last factor in Eq. (8) goes to unity and we recover the known bulk correlation function [2] (as we do in the noninteracting case $K_c = K_s = 1$).

To understand the physical implications of the boundary correlation function we study the *local* spectral density $N(\omega, r)$, which is given in terms of the Green's function as

$$N(\omega, r) \equiv \frac{1}{2\pi} \int_{-\infty}^{\infty} e^{i\omega t} \langle \{ \Psi_\sigma^\dagger(r, 0), \Psi_\sigma(r, t) \} \rangle dt, \quad (9)$$

where ω is measured relative to the Fermi energy and r is the distance from the boundary. Without the boundary,

this integral can be done exactly [11] with the result that the spectral density scales at the Fermi surface as $N(\omega) \propto |\omega|^\alpha$, where the exponent in the bulk is given by

$$\alpha = (K_c^2 + K_c^{-2} + K_s^2 + K_s^{-2})/4 - 1. \quad (10)$$

However, the boundary clearly has an effect on this exponent, and simple power counting shows that we expect a crossover to a boundary dominated regime for $\omega < v_\nu/r$ with a novel exponent $\alpha_B = (K_c^{-2} + K_s^{-2})/2 - 1$. Interestingly, the boundary exponent α_B therefore *always* dominates for sufficiently small ω . Moreover, we notice that the last two terms in Eq. (7) make a contribution which oscillates at twice the Fermi wave vector and drops off with the distance from the boundary proportional to $e^{i2k_F r} r^{-(K_c^2 + K_s^2)/2}$. This contribution is reminiscent of a Friedel oscillation, although it can probably not be observed directly, since experimental measurements of the density of states (e.g., photoemission) will average over several lattice sites. We therefore ignore those "Friedel" terms in the following calculations.

As an example, we consider the low-temperature Hubbard model away from half filling, which is well understood in terms of the TL model [2]. In this case, the SU(2) invariance forces $K_s = 1$, and it is known from Bethe ansatz calculations that $K_c^2 \rightarrow 1/2$ as $U \rightarrow \infty$ [12]. From these numbers, the well known result $N(\omega) \propto \omega^{1/8}$ for small ω follows immediately for the bulk regime $\omega \gg v_c/r$. In the presence of the boundary, however, we cross over to the boundary exponent $\alpha_B = 1/2$ for $\omega < v_c/r$. After rescaling the variable of integration in Eq. (9), we see that the spectral density is a function of the scaling variable $r\omega$ only (up to an overall constant): $N(r, \omega) = r^{-1/8} f(r\omega)$. After a deformation of the integration contour, a numerical integration of Eq. (9) is straightforward (we subtract the divergent part). The results in Fig. 1 clearly show the crossover from boundary behavior for $r\omega/v_c < 1$ with exponent $\alpha_B = 1/2$ to bulk behavior for $r\omega/v_c > 1$ with exponent $\alpha = 1/8$ (the corresponding power laws are superimposed). The observed

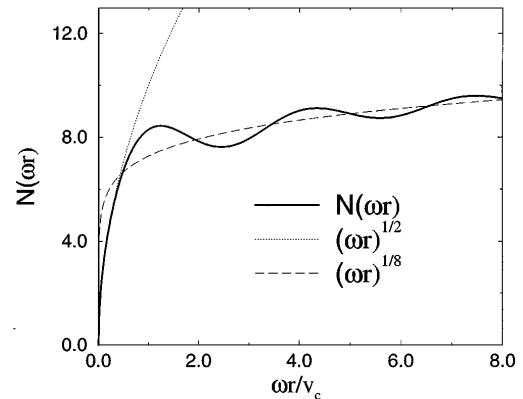


FIG. 1. The spectral density as a function of $r\omega$ in arbitrary units. The corresponding power laws for $\alpha = 1/8$ and $\alpha_B = 1/2$ are also shown.

oscillations in Fig. 1 are an interesting secondary effect, which vanish asymptotically as $\sin(2\omega r/v_c)(\omega r)^{-13/16}$ [but those are *not* due to the ‘‘Friedel’’ terms in Eq. (7) which have been neglected].

Our results have direct relevance for photoemission experiments on quasi-1D metals. At low temperatures the photoemission intensity $I(\omega)$ is proportional to the local spectral density $N(\omega, r)$, integrated over the region of escaping electrons and weighted by the Fermi-Dirac distribution $f_{\text{FD}}(\omega)$:

$$I(\omega) \propto \int dr f_{\text{FD}}(\omega) N(\omega, r). \quad (11)$$

[We neglect the small thermal shift in $N(\omega, r)$ at low temperatures.]

In a boundary dominated region, $I(\omega)$ is seen to be dramatically reduced at the Fermi level compared to a ‘‘bulk region.’’ Moreover, the finite energy resolution Δ of the photon lines effectively introduces an averaging over the ‘‘true’’ spectral density

$$I(\omega)_{\text{obs}} \equiv \frac{1}{\sqrt{2\pi}\Delta} \int e^{-(\omega-x)^2/2\Delta^2} I(x) dx. \quad (12)$$

This averaging completely wipes out the power-law singularities in either the bulk or the boundary case as shown in Fig. 2, where we plotted $I(\omega)_{\text{obs}}$ in arbitrary units at $T = 50$ K for boundary ($\alpha_B = 1/2$) and bulk ($\alpha = 1/8$) regimes, respectively, assuming an experimental resolution of $\Delta = 20$ meV (experimental values according to [5]). The corresponding three-dimensional case ($\alpha = 0$) is also shown for comparison. In the neighborhood of the Fermi level the observed boundary dominated spectral density appears to be depleted with an exponent of one or larger (compared to the exponent $\alpha = 1/8$ of the bulk spectral function without temperature or averaging effects).

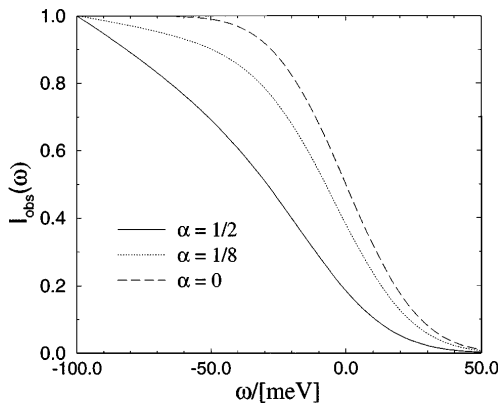


FIG. 2. The predicted intensity I_{obs} in arbitrary units as a function of ω for boundary and bulk cases (i.e., for power laws with $\alpha_B = 1/2$ and $\alpha = 1/8$, respectively). The corresponding three-dimensional case ($\alpha = 0$) is also shown. Temperature ($T = 50$ K) and finite resolution ($\Delta = 20$ meV) effects have been taken into account according to Eqs. (11) and (12).

In experiments the condition for boundary behavior $\omega < v_c/r$ will be fulfilled over an energy range $\omega \sim E_F/\ell$, where ℓ is the distance from the boundary in units of the lattice spacing. This means that if the effective length ℓ of the 1D chains is about one hundred lattice spacings, the boundary effects are observed over a region of $\lesssim 100$ meV around the Fermi energy (e.g., corresponding to an ‘‘impurity’’ density of 1% close to the cleaved surface). Turning to the photoemission data reported in [5], a combination of boundary effects and a finite experimental resolution go a long way to account for the observed suppression of spectral weight at the Fermi level. The experiments indeed suggest a scaling $I(\omega)_{\text{obs}} \propto \omega^{\alpha_{\text{obs}}}$ with $\alpha_{\text{obs}} > 1$ extending, however, over a larger energy interval, and some additional mechanism (e.g., long-range interactions [5,11] or electron-phonon coupling [13]) may have to be invoked to fully explain the data. Another way of directly examining the boundary region would be to probe the single crystal face where the open ends of the chains are. Since the electrons have an escape depth of only a few lattice spacings, the boundary exponent should be observable over a much larger energy range.

As a second example of the effect of open boundaries, we consider the momentum distribution of a *finite* system with length L and open boundary conditions, which can be expressed in terms of the chiral Green’s function

$$n(k, L) \equiv \frac{1}{L} \int_0^L dx dy \cos k(x-y) G(x, y, 0), \quad (13)$$

where k is measured relative to the Fermi wave vector k_F [we also implicitly subtract $n(0, L)$ to remove any divergences]. The bulk behavior can be determined by taking $L \rightarrow \infty$ and by simple power counting we see that $n(k, \infty) \propto |k|^\alpha$, where α is again given in Eq. (10). However, boundary effects will be present, and moreover we have to consider that we are now dealing with a *finite* system (i.e., open boundary conditions both at $x = 0$ and $x = L$). One way of determining the correct correlation functions in this case is to assume conformal invariance in the complex plane $z' = x + iv_\nu \tau$ (which is justified in the low-energy, long-wavelength limit and with decoupled spin and charge sectors). We then simply perform a conformal transformation onto a cylinder with circumference $2L$: $z' \rightarrow e^{i\pi z'/L}$ [after the analytic continuation in Eq. (6)]. Since we know the chiral Green’s function in the plane (z'), we immediately obtain the result for the finite case [14] (using the transformation rules for primary fields)

$$G(x, y, t) \propto - \prod_{\nu=c,s} \left(\frac{2L}{\pi} \sin \frac{\pi(\nu_\nu t + x - y)}{2L} \right)^{-(K_\nu + K_\nu^{-1})^2/8} \\ \times \left(\frac{2L}{\pi} \sin \frac{\pi(\nu_\nu t - x - y)}{2L} \right)^{-(K_\nu - K_\nu^{-1})^2/8} \\ \times \left(\frac{\sin \frac{\pi x}{L} \sin \frac{\pi y}{L}}{\sin \frac{\pi(\nu_\nu t + x + y)}{2L} \sin \frac{\pi(\nu_\nu t - x - y)}{2L}} \right)^{(K_\nu^{-2} - K_\nu^2)^2/8}. \quad (14)$$

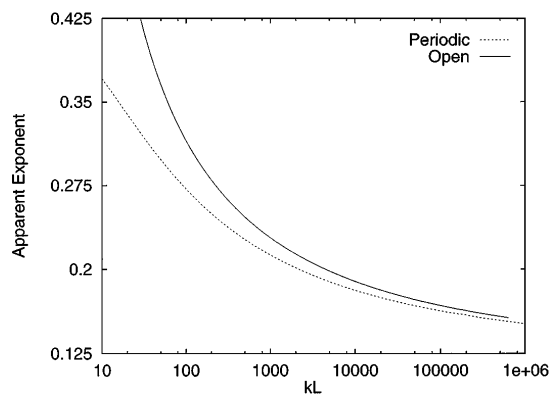


FIG. 3. The apparent exponent α_{app} of the momentum distribution for a finite system as a function of kL according to Eq. (13). As $kL \rightarrow \infty$, the bulk exponent $\alpha = 0.125$ is slowly approached.

We expect the critical behavior to be changed dramatically by this transformation, but now the exponent cannot be determined by simply counting the powers in the finite Fourier transform. Again, the momentum distribution is a function of a scaling variable kL only up to an overall constant $n(k, L) = L^{-\alpha} f(kL)$. We are mostly interested in the *apparent* critical exponent α_{app} near the Fermi wave vector $n(k, L) \propto |k|^{\alpha_{\text{app}}}$. This apparent exponent will change slowly depending on the scale kL at which we probe the system, so it is useful to define a scale dependent exponent in terms of the logarithmic derivative

$$\alpha_{\text{app}}(kL) \equiv \frac{k}{n(k, L)} \frac{\partial n}{\partial k}(k, L). \quad (15)$$

As our example we consider the case of the large- U Hubbard model again. After calculating α_{app} numerically as shown in Fig. 3, we find that the crossover is extremely slow. Even for huge values of $kL \sim 10^6$ we are still considerably far away from the accepted bulk exponent $\alpha = 0.125$. Since k is assumed to be small compared to k_F , this means that even macroscopic samples of several centimeters will have a finite-size dominated momentum distribution near k_F . A slow crossover is also observed for a *periodic* (but finite) system, which is shown for comparison in Fig. 3. The observed behavior is therefore mostly a finite size effect, but systems with an *open* boundary condition show an even slower crossover.

In conclusion, we have shown that an open boundary has a pronounced influence on the observed critical exponents in quasi-one-dimensional metals. The spectral density was shown to be *always* dominated by the boundary exponent for frequencies close to the Fermi energy, which has direct consequences for the interpretation of photoemission experiments. The momentum distribution exhibits strong finite size and also boundary effects close to the Fermi wave vector and the crossover to “bulk” behavior is extremely slow.

We thank I. Affleck, A.A. Nersesyan, and K. Schönhammer for valuable discussions, and M. Grioni for correspondence about photoemission experiments. This research was supported in part by the Swedish Natural Science Research Council.

-
- [1] F.D.M. Haldane, J. Phys. C **14**, 2585 (1981).
 - [2] For a recent review, see J. Voit, Report No. cond-mat/9510014 (to be published).
 - [3] F.P. Milliken, C.P. Umbach, and R.A. Webb (to be published).
 - [4] B. Dardel, D. Malterre, M. Grioni, P. Weibel, Y. Baer, and F. Lévy, Phys. Rev. Lett. **67**, 3144 (1991); Y. Hwu, P. Alméras, M. Marsi, H. Berger, F. Lévy, M. Grioni, D. Malterre, and G. Margaritondo, Phys. Rev. B **46**, 13 624 (1992).
 - [5] B. Dardel, D. Malterre, M. Grioni, P. Weibel, Y. Baer, J. Voit, and D. Jérôme, Europhys. Lett. **24**, 687 (1993).
 - [6] P.W. Anderson, Phys. Rev. Lett. **64**, 1839 (1990).
 - [7] S. Eggert and I. Affleck, Phys. Rev. B **46**, 10 866 (1992); Phys. Rev. Lett. **75**, 934 (1995).
 - [8] S. Tomonaga, Prog. Theor. Phys. **5**, 544 (1950); J.M. Luttinger, J. Math. Phys. (N.Y.) **4**, 1154 (1963).
 - [9] For a collection of relevant papers, see *Bosonization*, edited by M. Stone (World Scientific, Singapore, 1994).
 - [10] J.M. Kosterlitz, J. Phys. C **7**, 1046 (1974).
 - [11] K. Schönhammer and V. Meden, Phys. Rev. B **47**, 16 205 (1993); **48**, 11 521(E) (1993); J. Voit, J. Phys. C **5**, 8305 (1993).
 - [12] E.H. Lieb and F.Y. Wu, Phys. Rev. Lett. **20**, 1445 (1968).
 - [13] J. Voit and H.J. Schulz, Phys. Rev. B **37**, 10 068 (1988).
 - [14] Equation (14) agrees with an independent result by M. Fabrizio and A.O. Gogolin, Phys. Rev. B **51**, 17 827 (1995), where a finite-mode expansion of the boson was used instead.